

Chemical and Crystallographic Characterization of the Tip Apex in Scanning Probe Microscopy

Thomas Hofmann,* Florian Pielmeier, and Franz J. Giessibl

Institute of Experimental and Applied Physics, University of Regensburg, D-93053 Regensburg, Germany

(Dated: March 14, 2019)

The apex atom of a W scanning probe tip reveals a non-spherical charge distribution as probed by a CO molecule bonded to a Cu(111) surface [Welker *et al.* Science, 336, 444 (2012)]. Three high-symmetry images were observed and related to three low-index crystallographic directions of the W bcc crystal. Open questions remained, however, including the verification that the tip was indeed W-terminated, and whether this method can be easily applied to distinguish other atomic species. In this work, we investigate bulk Cu and Fe tips. In both cases we can associate our data with the fcc (Cu) and bcc (Fe) crystal structures. A model is presented, based on the partial filling of d orbitals, to relate the AFM images to the angular orientation of the tip structure.

The front atom of the tip in a scanning probe microscope is important - it can be compared to the objective lens in an optical microscope. In scanning tunneling microscopy (STM), the tip can often be treated as spherically symmetric (Tersoff-Hamann s-wave model [1]). In atomic force microscopy, the front atom strongly affects both the appearance of imaged atoms [2] as well as force spectroscopy [3]. An indirect method to determine the tip cluster is the comparison of experimental results with *ab initio* calculations for different realistic tip models [4–6]. Another possibility is the combination of field ion microscopy (FIM), which can resolve the atomic structure of a sharp asperity [7], with an AFM [8, 9]. A common method is the functionalization of the tip apex with atoms or molecules picked up from the surface [10–14]. Carbon monoxide (CO) is commonly used, because its confined and closed-shell electronic structure makes it an inert probe for high-resolution atomic force imaging [10–12, 15]. Recently, a CO molecule, adsorbed on a Cu(111) surface, has been used to probe the apex atom of a W tip [2] - a technique referred to as **CO Front atom Identification** (COFI) [3].

In this Letter, we show that COFI images and force spectroscopy can be used to distinguish Cu front atoms from W and Fe front atoms and to determine their angular orientation. We further introduce an electrostatic model that relates the symmetries of experimental COFI images to the partial filling of d-orbitals in the apex atom.

All measurements were performed in a low temperature STM/AFM operated at 4.4 K (LT STM/AFM, Omicron Nanotechnology, Taunusstein). The microscope is equipped with a qPlus sensor [16] and operated in the frequency modulation mode ($A = 50$ pm). We use qPlus sensors with tips etched from a Cu (99.95 %), a Fe (99.998 %) and a W (99.95 %) wire. The measurements are conducted on a Cu(111) sample, which is covered by about 0.01 ML CO. Prior to the measurements on the CO/Cu(111) sample, all tips are cleaned by field evaporation.

Tips normally show stable tunneling conditions upon the first approach on the sample, which indicates that the

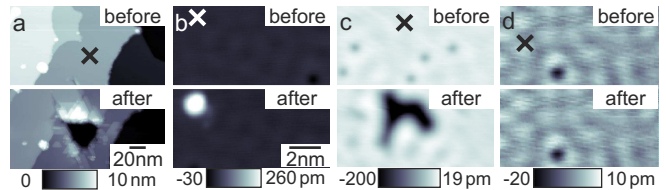


FIG. 1. (color online). Overview images of the Cu(111) surface before and after a tip poke event. The poke position is marked by a cross. a) A strong poke, where the tip is indented several nm into the surface, leads to a crater with a depth of a few nm. During a soft poke, in contrast, the tip is indented less than a nm. A small protrusion (b) or depression (c) are possible results. In rare cases no change (d) of the Cu surface is observed, although the tip cluster has apparently changed its orientation.

tip exposes a clean metal surface. The tip apex is then modified by poking it into the Cu surface. We distinguish two kinds of pokes. Indenting the tip several nanometers into the sample surface is a strong poke. In scanning probe microscopy this is a standard procedure to prepare tips [14, 17, 18] and leads to a crater in the sample surface with a depth of several nanometers [Fig. 1(a)]. During this procedure, sample material is transferred onto the tip, covering the whole tip apex with sample material [17, 19].

In contrast to these strong pokes, soft pokes can be performed to only modify the front-most part of the tip apex [2]. For that purpose, the tip is positioned above the clean Cu surface in STM feedback (100 pA, 10 mV). This conductivity corresponds to a distance of about 420 pm from quantum point contact [20]. Then the tip is approached between 400 to 900 pm and retracted, while a bias voltage between 0.5 and 5 V is applied. By far, the most common result of a soft poke are one or several small protrusions on the surface [Fig. 1(b)]. These consist of single or multiple atoms, which have been deposited from the tip. In some cases, a small indentation with a depth of a few hundred picometers is found, which indicates that a small amount of atoms is picked up from the sam-

ple [Fig. 1(c)]. These do not necessarily stick to the tip apex. In rare cases we do not observe any change of the sample surface after a soft poke, although the tip cluster has apparently changed its orientation [Fig. 1(d)].

During the measurements with the bulk Cu tips, the tip apex was modified by soft and hard pokes over thirty times. After each poke, the tip atom was characterized by COFI [2, 3]. This involves the tip being scanned at close distance over the CO molecule, while the averaged force gradient $\langle k_{ts} \rangle$ is recorded. The $\langle k_{ts} \rangle$ maps are referred to as the COFI images in the following. Among these COFI images [20] three high-symmetry images are identified (Fig. 2). Two are circular symmetric [Fig. 2(b) and 2(g)], the third one shows a twofold symmetry [Fig. 2(l)]. From the different contrast in the circular symmetric images, it is already apparent that they represent two different tip clusters. In addition, we obtained force-distance curves at certain positions in the COFI images. Those recorded in the center of the circular symmetric images [Fig. 2(e) and 2(j)] exhibit a large difference in the magnitude of the force (150 vs. 30 pN) and in the z -position of the attractive minimum and confirm that the COFI images represent two different tip clusters.

As in the case of the W tips [2], we can assign the three COFI images to the three low-index high-symmetry directions of a fcc crystal. The COFI images of the W tips are explained by calculations of the total charge density, which predict an increased charge density in direction of the nearest neighbors [21–23]. In contrast to W, calculations of the total charge density in bulk Cu only predict a spherical symmetric electron distribution [24–27], which would lead to a directionally independent interaction. Therefore we developed a tip model, which reproduces the COFI images and allows their unambiguous assignment to the crystallographic directions of the fcc lattice.

Density functional calculations of metal tips show that the Smoluchowski effect [28] leads to a surface dipole at the tip atom [5]. For a Cu adatom on a Cu(111) surface the same effect has been reported [17] and calculations show that the occupation of the 4s and 3d orbitals is reduced compared to an isolated Cu atom [29]. Therefore we model the Cu tip atom by partially occupied 3d orbitals and a positive point charge in the center. The spherical 4s orbital cannot explain the directionality in the COFI images and is therefore neglected.

In an isolated atom, the 3d orbitals are degenerate and their occupation is equal. In the case of a tip atom, the degeneracy is lifted according to crystal field theory [30]. The reason is that the partially unscreened nuclei of the nearest neighbors generate a nonuniform attractive potential [31, 32]. For each 3d orbital the shift of the energy level and, as a result, its occupation can be estimated by its angular overlap with all nearest neighbors [33] (details in Ref. [20]). As an effect, the occupation of the five different 3d orbitals varies, with the maximal occupation

limited to 2 e (Fig. 2).

Following the arguments in Ref. [2], we estimate the interaction of the tip atoms with the CO molecule by electrostatics [34]. The CO molecule is considered as a dipole with a negative charge on the oxygen atom and a realistic dipole moment of $0.1 \text{ e} \cdot 100 \text{ pm}$ [35, 36]. In order to approximately match the contrast in the COFI images and the characteristics of the force-distance curves, the positive charge in the center of the model tip atom is adjusted. For all tip orientations the total charge of the model tip atom $\Delta = Q_{\text{core}} - Q_{\text{3d elec.}}$ is positive, with $\Delta_{100} = +0.25 \text{ e}$, $\Delta_{111} = +0.52 \text{ e}$ and $\Delta_{110} = +0.04 \text{ e}$.

The calculated image of the Cu(100) tip shows a circular symmetry with a strong attraction in the center [Fig. 2(d)], whereas the image of the Cu(111) tip only reveals a small attractive dip [Fig. 2(i)]. We therefore assign the COFI images in Fig. 2(b) and 2(g) to a Cu(100) and a Cu(111) tip, respectively. The calculation for the Cu(110) tip [Fig. 2(n)] yields a twofold symmetric image similar to the COFI image in Fig. 2(l). Notably, the experimental tip image is more than 2.5 times the size of the calculated images. This is explained by the bending of the CO molecule that is known to magnify the image of the tip atom [3] or the length of intermolecular bonds [37] and is not considered in the calculations.

In the graphs in Fig. 2(e), 2(j) and 2(o) we find that the calculation yields force-distance curves that approximately reproduce the experimental curves. The deviation can be explained by neglecting the contributions of the 4s and the core shells. Additionally, the calculation of the interaction between the CO and the metal tip does not include Pauli repulsion, which occurs at small tip-sample distances [10, 38].

The measurements with Fe tips again reveal three high-symmetry COFI images [Figs. 3(b), 4(c) and 4(d)]. These exhibit the same symmetries as the W tips [Figs. 3(a), 4(a) and 4(b)] and are therefore assigned to tips oriented in $\langle 100 \rangle$, $\langle 110 \rangle$ and $\langle 111 \rangle$ direction. Although iron has partially filled d shells, calculations of the total charge density in the bulk or on the surface do not show a higher electron density in direction of the nearest-neighbors [39, 40]. Therefore we expect that, as in the case of Cu, a partial depletion of the d states is responsible for the directional dependent interaction with CO.

In order to evaluate the potential of the COFI method to distinguish between different chemical species at the tip apex, we compare COFI images and force-distance curves of Cu, Fe and W tips. The comparison is divided into tips, whose COFI image is circular symmetric (Fig. 3), and tips that exhibit a two- or threefold symmetry (Fig. 4).

Circular symmetric COFI images are observed for W, Fe and Cu tips, oriented in $\langle 100 \rangle$ -direction, and Cu(111) tips [Fig. 3(a)-(d)]. The Cu(111) tip can easily be distinguished from all $\langle 100 \rangle$ tips by the contrast in the COFI images and its force-distance curve [Fig. 3(e)]. The COFI

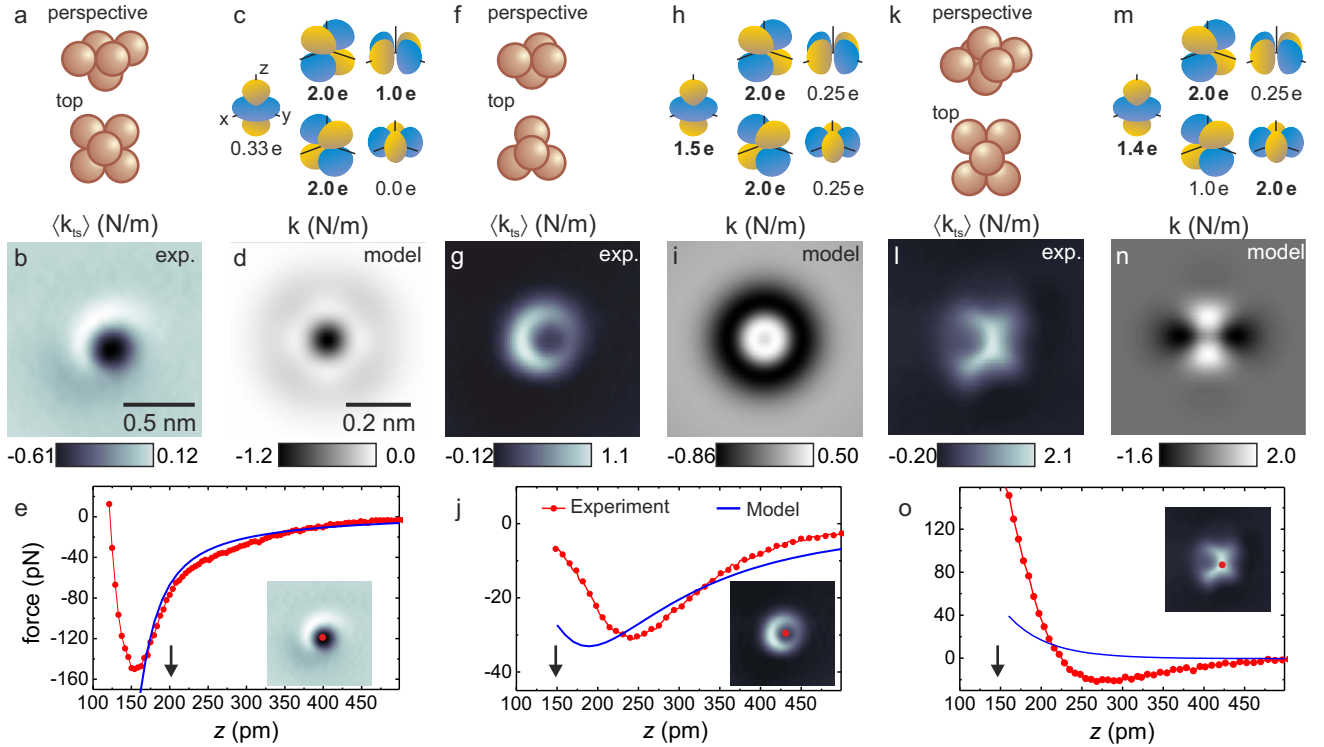


FIG. 2. (color online). Cu tips yield three high-symmetry COFI images (b, g and l), which can be assigned to Cu tip clusters pointing into the $\langle 100 \rangle$ (a), $\langle 111 \rangle$ (f) and $\langle 110 \rangle$ directions (k). To justify the assignment, we develop a model for the tip atom and calculate its electrostatic interaction with the dipole of the CO molecule. The model tip atom consists of a positive charge in the center, surrounded by unequally occupied 3d orbitals. Their occupation (c, h and m) is determined by their angular overlap with the nearest neighbors. The central charge is adjusted that the contrast in the model images, calculated at a core-core distance of 200 (d), 145 (i) and 160 pm (n), and the force-distance behavior (e, j and o) approximately fits the experimental results. Note that the experimental tip-sample distance and the core-core distance in the model are chosen to be equal. The black arrows in the force-distance graphs indicate the distance of the COFI image.

images of the $\langle 100 \rangle$ tips, on the other hand, do not allow a discrimination. The force-distance curves obtained with three different Cu $\langle 100 \rangle$ tips, however, show a significant smaller maximal attractive force (130 – 150 pN, variation explained in [20]) than those obtained with Fe $\langle 100 \rangle$ and W $\langle 100 \rangle$ tips (≈ 250 pN). It is therefore possible to distinguish Cu from Fe and W tips for the $\langle 100 \rangle$ orientations. To support this finding, we modified a W tip apex by several hard pokes into the Cu surface. The COFI image after the modification revealed the image of a tip oriented in $\langle 100 \rangle$ direction. The comparison of its force-distance curve [black line in Fig. 3(e)] with curves of Cu $\langle 100 \rangle$ and W $\langle 100 \rangle$ tips clearly reveals a decoration of the W tip apex with Cu. This is expected for such tip treatment [17, 19] and proves the capability of COFI to identify a contamination of the tip apex with Cu.

In Fig. 4, examples of COFI images of W, Fe and Cu tips with two- and threefold symmetry are presented. COFI images of W, Fe and Cu tips, oriented in $\langle 110 \rangle$ -direction are all twofold symmetric, but the image of the Cu tip [Fig. 4(e)] is significantly different from those of W [Fig. 4(a)] and Fe [Fig. 4(c)]. The Cu tip image features

a repulsive part with the shape of a 'rooftop' with four shallow minima, whereas the W/Fe tip images exhibit a repulsive bar with two attractive minima. Therefore a Cu $\langle 110 \rangle$ tip can be unambiguously identified by the COFI image. As expected, W and Fe tips cannot be distinguished from the qualitative COFI image, as both are bcc crystals.

For this purpose, we analyze the force-distance curves of the two- and threefold symmetric tips [Fig. 4(f)], recorded at the repulsive maximum in the COFI images. We find that curves, recorded with different W $\langle 110 \rangle$ and W $\langle 111 \rangle$ tips, are almost identical, exhibiting a force minimum between 30 and 35 pN. The curves of the Fe $\langle 110 \rangle$ and Fe $\langle 111 \rangle$ tips, on the other hand, show a smaller attractive minimum of 15 to 22 pN. Therefore Fe and W can be distinguished with the help of the force-distance curves. The greater deviation between the force minimum of the Fe $\langle 110 \rangle$ and Fe $\langle 111 \rangle$ tips is probably due to a greater misalignment to the precise $\langle 110 \rangle$ and $\langle 111 \rangle$ orientations. The angular deviations are smaller for the W tips shown in Fig. 4(a) and 4(b). For details on the effect of angular alignments, see Fig. S9 in [2].

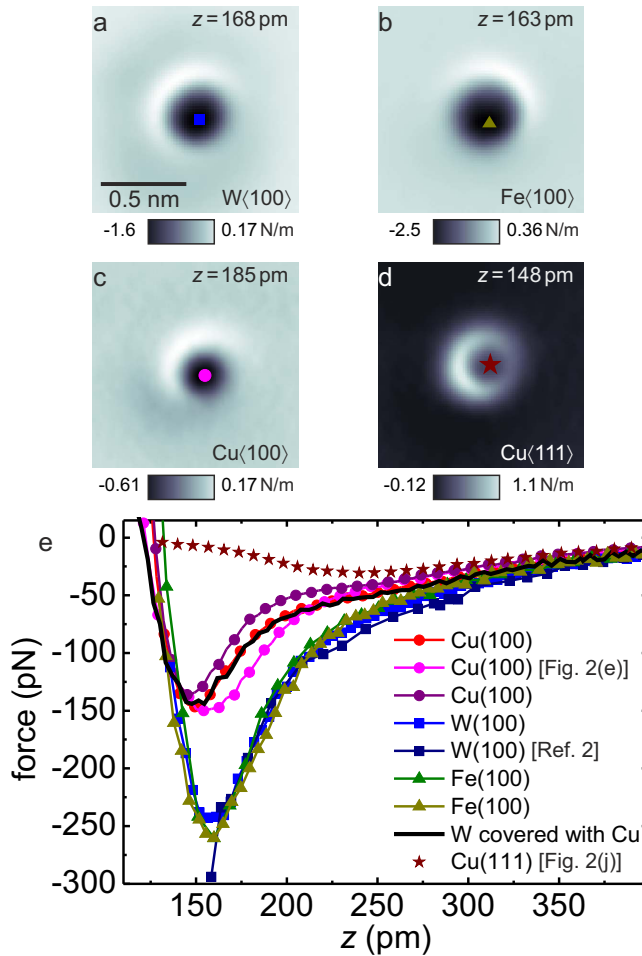


FIG. 3. (color online). Comparison of W (a), Fe (b) and Cu tips (c and d), which show a circular symmetry in the COFI image (c and d are the same as in Fig. 2). e) Force-distance curves of W<100> (squares), Fe<100> tips (triangles), Cu<100> (circle) and Cu<111> tips (stars). The solid (black) line represents a W tip, which is contaminated with Cu.

In conclusion, we report three high-symmetry COFI images for Cu and Fe, which can be related to the high-symmetry directions of the fcc and bcc crystals. We therefore suggest that in almost all cases the tip clusters exhibit a bulk-like crystal structure. A tip model based on the partial depletion of selected d orbitals can qualitatively explain the observed COFI images. However, for a quantitative description *ab initio* calculations may be helpful, similar to those for the results with W tips [41]. The comparison of the results for W, Fe and Cu tips reveals, that COFI is a powerful method to distinguish between the orientation as well as the chemical species of the tip atom. The method has been proven to be useful for measurements on various samples like Si [3], NiO [42] and graphene [43].

The authors thank Alfred J. Weymouth and Jascha Repp for discussions and kindly acknowledge finan-

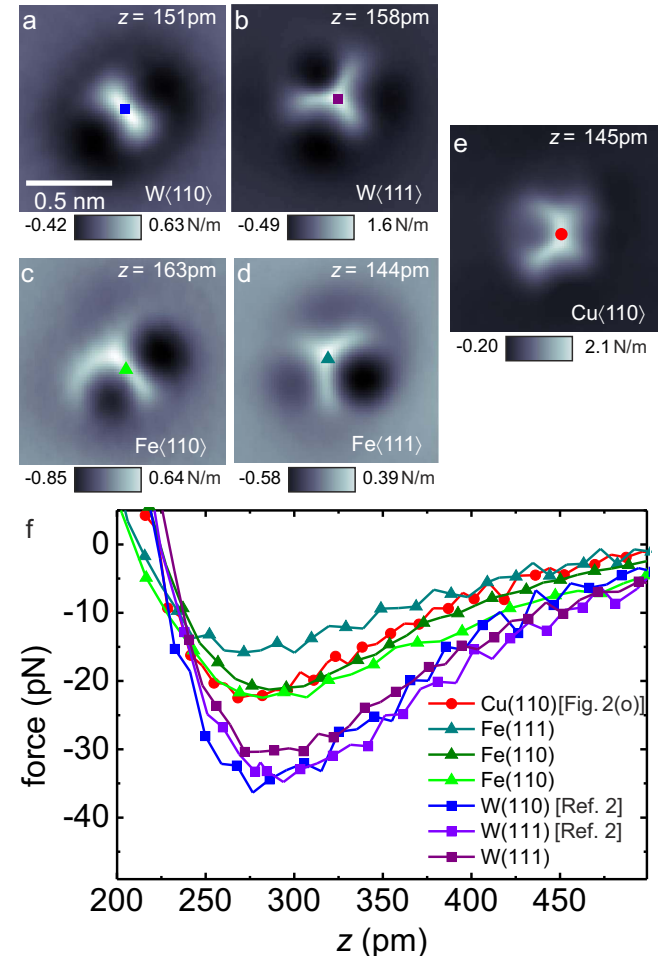


FIG. 4. (color online). Comparison of W, Fe and Cu tips revealing two- or threefold symmetry. a-e) COFI images of the corresponding W (a, b), Fe (c, d) and Cu tips (e) (a is reproduced from [2], e is the same as in Fig. 2(i)). f) Force-distance curves of several W, Fe and Cu tips.

cial support from the Deutsche Forschungsgemeinschaft (Grant No. GRK 1570).

* thomas.hofmann@physik.uni-regensburg.de

- [1] J. Tersoff and D. R. Hamann, Physical Review Letters **50**, 1998 (1983).
- [2] J. Welker and F. J. Giessibl, Science **336**, 444 (2012).
- [3] J. Welker, A. J. Weymouth, and F. J. Giessibl, ACS Nano **7**, 7377 (2013).
- [4] Y. Sugimoto, P. Pou, M. Abe, P. Jelinek, R. Pérez, S. Morita, and O. Custance, Nature **446**, 64 (2007).
- [5] G. Teobaldi, K. Lämmle, T. Trevethan, M. Watkins, A. Schwarz, R. Wiesendanger, and A. L. Shluger, Physical Review Letters **106**, 216102 (2011).
- [6] M. Ternes, C. González, C. P. Lutz, P. Hapala, F. J. Giessibl, P. Jelinek, and A. J. Heinrich, Physical Review Letters **106**, 016802 (2011).

[7] E. W. Müller, *Zeitschrift für Physik* **131**, 136 (1951).

[8] J. Falter, G. Langewisch, H. Hölscher, H. Fuchs, and A. Schirmeisen, *Physical Review B* **87**, 115412 (2013).

[9] W. Paul, D. Oliver, Y. Miyahara, and P. H. Grütter, *Physical Review Letters* **110**, 135506 (2013).

[10] L. Gross, F. Mohn, N. Moll, P. Liljeroth, and G. Meyer, *Science* **325**, 1110 (2009).

[11] N. Pavliček, B. Fleury, M. Neu, J. Niedenführ, C. Herranz-Lancho, M. Ruben, and J. Repp, *Physical Review Letters* **108**, 086101 (2012).

[12] M. P. Boneschanscher, J. van der Lit, Z. Sun, I. Swart, P. Liljeroth, and D. Vanmaekelbergh, *ACS Nano* **6**, 10216 (2012).

[13] G. Kichin, C. Wagner, F. S. Tautz, and R. Temirov, *Physical Review B* **87**, 081408 (2013).

[14] F. Mohn, B. Schuler, L. Gross, and G. Meyer, *Applied Physics Letters* **102**, 073109 (2013).

[15] Z. Sun, M. P. Boneschanscher, I. Swart, D. Vanmaekelbergh, and P. Liljeroth, *Physical Review Letters* **106**, 046104 (2011).

[16] F. J. Giessibl, *Applied Physics Letters* **73**, 3956 (1998).

[17] L. Limot, J. Kröger, R. Berndt, A. García-Lekue, W. Hofer, and J. Kröger, *Physical Review Letters* **94**, 126102 (2005).

[18] G. Schull, T. Frederiksen, A. A. Arnaud, D. Sánchez-Portal, R. Berndt, and D. Sánchez-Portal, *Nature nanotechnology* **6**, 23 (2011).

[19] S.-W. Hla, K.-F. Braun, V. Iancu, and A. Deshpande, *Nano Letters* **4**, 1997 (2004).

[20] T. Hofmann, F. Pielmeier, and F. J. Giessibl, “Supplemental Information”.

[21] M. Posternak, H. Krakauer, A. Freeman, and D. Koelling, *Physical Review B* **21**, 5601 (1980).

[22] L. Mattheiss and D. Hamann, *Physical Review B* **29**, 5372 (1984).

[23] C. A. Wright and S. D. Solares, *Nano letters* **11**, 5026 (2011).

[24] C. Fong, J. Walter, and M. Cohen, *Physical Review B* **11**, 2759 (1975).

[25] J. Gay, J. Smith, and F. Arlinghaus, *Physical Review Letters* **38**, 561 (1977).

[26] A. Euceda, D. Bylander, L. Kleinman, and K. Mednick, *Physical Review B* **27**, 659 (1983).

[27] A. Euceda, D. Bylander, and L. Kleinman, *Physical Review B* **28**, 528 (1983).

[28] R. Smoluchowski, *Physical Review* **60**, 661 (1941).

[29] J. A. Rodriguez and M. Kuhn, *The Journal of Physical Chemistry* **98**, 11251 (1994).

[30] J. Van Vleck, *Physical Review* **41**, 208 (1932).

[31] P. Rao and J. Waber, *Surface Science* **28**, 299 (1971).

[32] J. Herbst, *Physical Review B* **15**, 3720 (1977).

[33] C. E. Schäffer and C. K. Jørgensen, *Molecular Physics* **9**, 401 (1965).

[34] R. Feynman, *Physical Review* **56**, 340 (1939).

[35] Z. Zuo, W. Huang, P. Han, and Z. Li, *Journal of molecular modeling* **15**, 1079 (2009).

[36] M. Feng, P. Cabrera-Sanfelix, C. Lin, A. Arnaud, D. Sánchez-Portal, J. Zhao, P. M. Echenique, and H. Petek, *ACS nano* **5**, 8877 (2011).

[37] L. Gross, F. Mohn, N. Moll, B. Schuler, A. Criado, E. Gutián, D. Peña, A. Gourdon, and G. Meyer, *Science* **337**, 1326 (2012).

[38] N. Moll, L. Gross, F. Mohn, A. Curioni, and G. Meyer, *New Journal of Physics* **12**, 125020 (2010).

[39] C. Wang and A. Freeman, *Physical Review B* **24**, 4364 (1981).

[40] R. Wu and A. Freeman, *Physical Review B* **47**, 3904 (1993).

[41] C. A. Wright and S. D. Solares, *Journal of Physics D: Applied Physics* **46**, 155307 (2013).

[42] F. Pielmeier and F. J. Giessibl, *Physical Review Letters* **110**, 266101 (2013).

[43] T. Hofmann, A. J. Weymouth, A. Donarini, and F. J. Giessibl, in preparation.